Journal of the Ceramic Society of Japan 123 [10] 967-971 2015 Paper

Double-layer dye-sensitized solar cells using $SrTiO_3$ and $BaTiO_3$ second layer with enhanced photovoltaic performance

Yuji OKAMOTO* **and Yoshikazu SUZUKI*,**,†**

*Graduate School of Pure and Applied Sciences, University of Tsukuba, Ibaraki 305–8573, Japan
**Faculty of Pure and Applied Sciences, University of Tsukuba, Ibaraki 305–8573, Japan

Double-layer electrodes using TiO_2-P25 as the first layer and $SrTiO_3$ or $BaTiO_3$ as the second layer were prepared to improve photovoltaic performance of dye-sensitized solar cells (DSCs), since $SrTiO_3$ and $BaTiO_3$ have more negative conduction bands than that of TiO_2. TiO_2-anatase second layer with the similar particle size to these double oxides was also prepared as a comparison. Crystal structure, microstructure, film thickness, amount of dye adsorption, *J–V* curves and IPCE spectra were characterized. Open-circuit voltage (V_{OC}) of the DSCs with the $SrTiO_3$ or $BaTiO_3$ second layer was improved due to the inhibition of electron–hole recombination by the second layer at the top side of the TiO_2 first layer. Elongation of the electron life time due to the band-structure matching might be another reason of the increase in V_{OC}. By using the second layer, short-circuit current density (J_{SC}) was also slightly improved (∼4%), possibly due to the increase of electrode thickness and light confinement effect for >∼650 nm. As a result, the DSC using $BaTiO_3$ second layer electrode had the largest conversion efficiency of 5.71% with an enhancement of 11.3% compared to that of TiO_2-P25 single-layer electrode.

Key-words : $SrTiO_3$, $BaTiO_3$, Dye-sensitized solar cells, Double-layer electrode, Band-structure matching

[Received June 17, 2015; Accepted July 25, 2015]

1. Introduction

Dye-sensitized solar cells (DSCs) have attracted much attention because of their simple fabrication processes and fashionable colorful designs.[1] The photoelectric conversion efficiency of the advanced DSCs has exceeded 10%,[2)–8)] which is almost equal to that of amorphous Si solar cells. DSCs are composed of a dye-sensitized porous oxide electrode on a transparent conducting glass, an electrolyte and a Pt coated counter electrode.[9] To date, TiO_2-anatase nanoparticles are typically applied to the porous oxide electrodes. TiO_2 nanoparticles with large surface area can adsorb a great amount of dye molecules, giving a large light harvesting and an efficient electron injection.[10]

As a strategy to improve the efficiency of DSCs, double-layer electrodes, either same-compound (homo) or different-compound (hetero) layers, have been reported. Wang et al.[11] reported that a short-circuit current density (J_{SC}) was enhanced by using small and large TiO_2 nanoparticles for the first and second layers, respectively. The large particles in the second layer scattered the long-wavelength light over ∼650 nm, which increased the total light absorption, and resulted in increased J_{SC} (i.e., light confinement effect).

Other oxides, such as ZnO, SnO_2, Nb_2O_5 and WO_3, have also been studied as oxide electrode.[12)–22)] Recently, we have studied the performance of DSCs with perovskite-type $SrTiO_3$, $CaTiO_3$ and $BaTiO_3$ electrodes,[23] either monolithic perovskite or composites with TiO_2. In our previous study,[23] an increase of open-circuit voltage (V_{OC}) was realized, which was attributed to the modified band structure; these perovskite-type double oxides have larger difference between the conduction bands (CB) and electrolyte's redox potential than that of TiO_2-anatase, due to their more negative CB.[24)–26)] On the other hand, the more negative CB led to a decrease of electron injection from the dyes to oxide electrodes, resulting in smaller J_{SC} than TiO_2.[27]

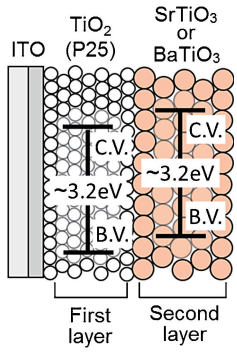

Fig. 1. Schematic illustration of double-layer electrode.

In this study, the double-layer electrodes were prepared to improve V_{OC}, J_{SC}, and the conversion efficiency; they are composed of nano-sized TiO_2-P25 (anatase and rutile mixture) as the first layer and $SrTiO_3$ or $BaTiO_3$ with relatively large particle size as the second layer (**Fig. 1**). The aims of this structure are as follows:

1) extended light path and light confinement by using the second layer (to improve J_{SC}),
2) inhibition of electron–hole recombination at the interface of first and second layers (to improve V_{OC}),
3) elongation of electron life time by the band structure matching (to improve V_{OC}).

2. Experimental

2.1 Preparation of $SrTiO_3$ and $BaTiO_3$ powders

In the same way as our previous report,[23] commercially availa-

† Corresponding author: Y. Suzuki; E-mail: suzuki@ims.tsukuba.ac.jp

DOI http://dx.doi.org/10.2109/jcersj2.123.967

ble $SrCO_3$ and $BaCO_3$ powders (99.9%, Wako Pure Chemical Industries Ltd., Osaka, Japan) were used as SrO and BaO sources. TiO_2-anatase powder (99%, Kojundo Chemical Laboratory Co. Ltd., Saitama, Japan) was used for TiO_2 source. Each carbonate powder and TiO_2 powder (1:1 in molar fraction) were mixed by wet-ball milling with nylon balls including steel core for 2 h in ethanol. The slurries were dried by a vacuum evaporator for 30 min and then, additionally dried in an oven at 80°C for 24 h. The mixed powders were molded to cylindrical pellets by a uniaxial press at 11.3 MPa to enhance the reactivity. The pellets were sintered at 1200°C for 2 h in air. After cooling, the pellets were crushed and planetary ball-milled in ethanol for 4 h to obtain $SrTiO_3$ and $BaTiO_3$ powders.

2.2 Preparation of double-layer DSC

The commercial TiO_2-P25 powder with ~30 nm particle size (Nippon Aerosil Co., Ltd., Tokyo, Japan) was used as the first layer. The TiO_2-P25 powder was mixed with polyethylene glycol (Molecular weight: 20,000, Wako Pure Chemical Industries Ltd., Osaka, Japan), distilled water, ethanol (99.5%, Wako Pure Chemical Industries Ltd., Osaka, Japan) and acetylacetone (99%, Wako Pure Chemical Industries Ltd., Osaka, Japan) by a magnetic stirrer for 30 min. The TiO_2-P25 paste was coated on indium-doped SnO_2 conducting glasses (ITO, Type 0052, 10 Ω/sq., Geomatec Co. Ltd., Yokohama, Japan) by a squeegee method with the electrode area of 1 cm^2. The coated electrodes were then dried on a hot-plate at 100°C for 10 min, and calcined at 450°C for 30 min. After cooling to room temperature, these electrodes were immersed in an 80 mM $TiCl_4$ solution (95%, Wako Pure Chemical Industries Ltd., Osaka, Japan) at 70°C for 30 min, rinsed with ethanol and finally dried in air. For comparison, DSC with TiO_2-P25 single-layer electrode and double-layer electrode (first layer: TiO_2-P25, second layer: TiO_2-anatase with the diameter of ~200 nm) were also prepared. After the $TiCl_4$ treatment, the TiO_2-P25 single-layer electrode and double-layer electrodes were calcined at 450°C for 60 min and 15 min, respectively. As for the double-layer electrodes, TiO_2-anatase, $SrTiO_3$ and $BaTiO_3$ pastes, prepared in the same manner as that of TiO_2-P25, were coated on the TiO_2-P25 films, and then calcined at 450°C for 45 min. After cooling to 80°C, these electrodes were immersed in a 0.5 mM N719 dye solution in ethanol (Sigma-Aldrich Co. LLC.) at 40°C for 24 h, and finally washed with ethanol.

The DSCs were assembled by placing the dye-sensitized electrodes on the counter electrodes of Pt-coated ITO glasses with a 50 µm polyethylene film spacers. The cells were clipped together as open cells. The electrolyte solution was composed of 0.05 M I_2 (99.9%, Wako Pure Chemical Industries Ltd., Osaka, Japan), 0.1 M LiI (97%, Wako Pure Chemical Industries Ltd., Osaka, Japan), 0.6 M 1,2-dimethyl-3-propylimidazolium iodide (>98%, Sigma-Aldrich Co. LLC), 0.5 M 4-*tert*-butylpyridine (TBP, 96%, Sigma-Aldrich Co. LLC.), in acetonitrile.

2.3 Characterization

X-ray diffraction (XRD, 40 kV, 40 mA, Multiflex, RIGAKU, Tokyo, Japan) was used to determine the crystal structure of synthesized $SrTiO_3$ and $BaTiO_3$ powders. Scanning electron microscopy (SEM, JSM-5600, JEOL Ltd., Tokyo, Japan) was applied to investigate morphology of the oxide powders and film thickness. Current density–voltage (J–V) characteristics was recorded with 6241A source meter (ADCMT, Tokyo, Japan) by using a solar simulator (XES-40S1, San-Ei Electric, Osaka, Japan) calibrated to AM 1.5, 100 mW/cm^2 with a standard silicon photodiode (BS520, Bunkoh-Keiki Co. Ltd., Tokyo, Japan). To measure the amounts of loaded dyes, the sensitized electrodes were immersed in a 0.1 M NaOH aq. solution for 6 h to desorb the dyes, and then, optical absorption spectra were measured by using ultraviolet–visible (UV–Vis) spectroscopy (UV3100PC, Shimadzu Co., Kyoto, Japan). Incident photon-to-current conversion efficiency (IPCE) was measured with a spectral response & IPCE measurement system (SM-250, Bunkoukeiki Co., Tokyo, Japan).

3. Results and discussion

3.1 Evaluation of synthesized double oxide powders

Figure 2 shows the XRD patterns of synthesized $SrTiO_3$ and $BaTiO_3$ powders. It is observed that single-phase cubic $SrTiO_3$ and tetragonal $BaTiO_3$ were obtained, respectively. ICDD-JCPDS No. 86-0178 for cubic $SrTiO_3$ and ICDD-JCPDS No. 74-4540 for tetragonal $BaTiO_3$ were used to determine the crystal structure. **Figure 3** demonstrates SEM images of the oxide powders used for the electrodes. The diameters of TiO_2-P25 (for the first layer), TiO_2-anatase (for the second layer), $SrTiO_3$ and $BaTiO_3$ particles were ~30, ~200, 200–500 nm and ~1 µm, respectively. The particle size of $SrTiO_3$ was smaller than that of $BaTiO_3$, as observed in the previous paper,[23] probably because the melting point of $SrTiO_3$ (~2080°C) is higher than that of $BaTiO_3$ (~1625°C).

3.2 Film thickness and dye adsorption

First of all, DSCs with (a) TiO_2-P25 single-layer electrode, (b) TiO_2-anatase double-layer electrode, (c) $SrTiO_3$ double-layer electrode and (d) $BaTiO_3$ double-layer electrode are named as TiO_2-P25, TiO_2-anatase/TiO_2-P25, $SrTiO_3$/TiO_2-P25 and $BaTiO_3$/

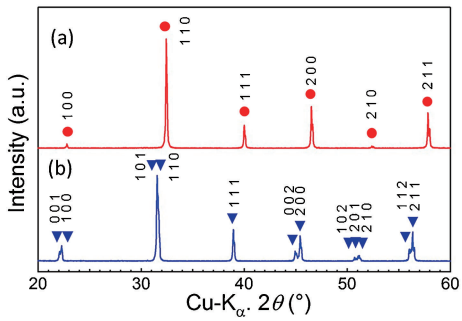

Fig. 2. XRD patterns of the synthesized (a) $SrTiO_3$ and (b) $BaTiO_3$ powders.

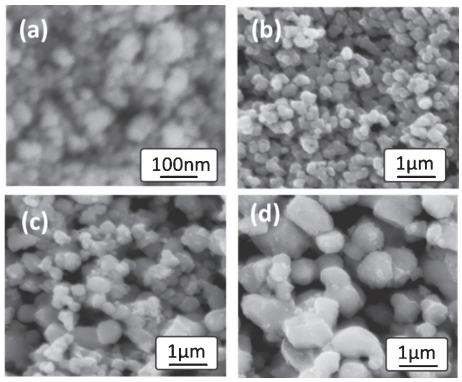

Fig. 3. SEM images of (a) TiO_2-P25, (b) TiO_2-anatase, (c) $SrTiO_3$ and (b) $BaTiO_3$ powders.

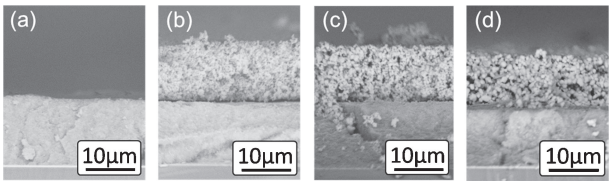

Fig. 4. SEM cross-section images of the oxide electrodes: (a) TiO_2-P25, (b) TiO_2-anatase/TiO_2-P25, (c) $SrTiO_3$/TiO_2-P25 and (d) $BaTiO_3$/TiO_2-P25.

Table 1. The amount of adsorbed dyes of (a) TiO_2-P25 single and double-layer electrodes (per area), (b) single-layer electrodes made from each oxide (per area per thickness)

(a) Sample	Adsorbed dyes (10^{-7} mol/cm^2)
TiO_2-P25	1.52
TiO_2-anatase/TiO_2-P25	1.44
$SrTiO_3$/TiO_2-P25	1.68
$BaTiO_3$/TiO_2-P25	1.39

(b) Sample	Adsorbed dyes (10^{-9} mol/cm^2·μm)
TiO_2-P25	12.96
TiO_2-anatase	1.05
$SrTiO_3$	3.36
$BaTiO_3$	2.01

Table 2. Photovoltaic output parameters of the DSCs using the single and double-layer electrodes

Sample	J_{SC} (mA/cm^2)	V_{OC} (mV)	FF	η (%)	R_s (Ω)	R_{sh} (kΩ)
TiO_2-P25	12.7	717	0.573	5.12	17.1	3.57
TiO_2-anatase/TiO_2-P25	13.2	724	0.574	5.49	16.3	2.90
$SrTiO_3$/TiO_2-P25	12.8	735	0.565	5.32	17.9	5.65
$BaTiO_3$/TiO_2-P25	13.2	744	0.582	5.71	17.0	4.18

TiO_2-P25, respectively. **Figure 4** shows the SEM cross-section images of these electrodes. It can be seen that thickness of the first layer (TiO_2-P25) was ~12–13 μm, and those of the second layers were ~10–11 μm.

As summarized in **Table 1**(a), the amounts of adsorbed dyes (per area) of TiO_2-P25, TiO_2-anatase/TiO_2-P25, $SrTiO_3$/TiO_2-P25 and $BaTiO_3$/TiO_2-P25 were 1.52×10^{-7}, 1.44×10^{-7}, 1.68×10^{-7} and 1.39×10^{-7} mol/cm^2, respectively. Despite the double-layer structure, total amounts of adsorbed dyes were almost constant in all electrodes. To verify this result, the amounts of adsorbed dyes of single-layer electrodes made of TiO_2-P25, TiO_2-anatase, $SrTiO_3$ and $BaTiO_3$ were further examined (per area per thickness) as shown in Table 1(b). These single-layer oxide films were prepared in the same manner as the TiO_2-P25 single-layer electrode. The dye adsorptions of TiO_2-anatase, $SrTiO_3$ and $BaTiO_3$ were smaller by one scale than that of TiO_2-P25. Hence, the second layers did not affect the total dye adsorption very much.

3.3 DSC performance

The J–V characteristics of the DSCs are shown in **Table 2** and **Fig. 5**. The J_{SC} of TiO_2-P25, TiO_2-anatase/TiO_2-P25, $SrTiO_3$/TiO_2-P25 and $BaTiO_3$/TiO_2-P25 were 12.7, 13.2, 12.8 and 13.2 mA/cm^2, respectively. The DSCs with double-layer electrodes had larger J_{SC} than that with single-layer electrode. The

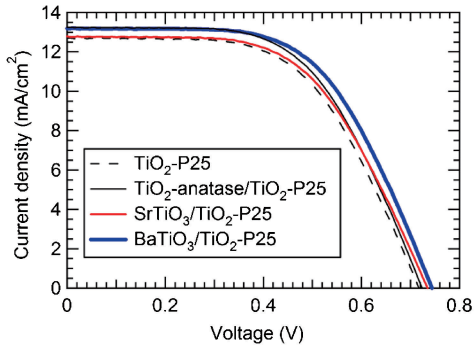

Fig. 5. J–V curves of DSCs composed of the single and double-layer electrodes at 100 mW/cm^2.

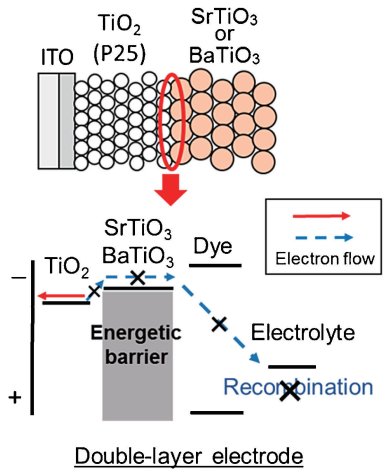

Fig. 6. Schematic diagram of the inhibition of recombination by the second layers of $SrTiO_3$ and $BaTiO_3$.

V_{OC} of the TiO_2-P25 and TiO_2-anatase/TiO_2-P25 were almost constant (717 and 724 mV), whereas that of $SrTiO_3$/TiO_2-P25 and $BaTiO_3$/TiO_2-P25 were enhanced to 735 and 745 mV, respectively. Judging from the results, the improvements of V_{OC} were attributed to the $SrTiO_3$ and $BaTiO_3$ second layers. To investigate the effect of the $SrTiO_3$ and $BaTiO_3$ second layers, a series resistance (R_s) and shunt resistance (R_{sh}) were calculated from the gradient of J–V curves at the V_{OC} and J_{SC},[28] respectively. R_s values of all DSCs were comparable. On the other hand, R_{sh} values of $SrTiO_3$/TiO_2-P25 and $BaTiO_3$/TiO_2-P25 (5.65 and 4.18 kΩ) were higher than those of TiO_2-P25 and TiO_2-anatase/TiO_2-P25 (3.57 and 2.90 kΩ). An enhanced R_{sh} shows a decrease of leakage and recombination of electrons, resulting in improvements of J_{SC} and V_{OC}.[28),29)]

Considering the structure of double-layer electrodes in this study (Fig. 1), the top side of the TiO_2-P25 film is substantially covered by the $SrTiO_3$ or $BaTiO_3$ second layer, whereas the top surface is completely exposed to the electrolyte in the single layer electrode. Therefore, the electron–hole recombination in the vicinity of the top side of TiO_2 layer is inhibited, due to more negative CB of $SrTiO_3$ and $BaTiO_3$ than that of TiO_2 (**Fig. 6**), which resulted in the increase of V_{OC}. Such a result was reported for the coated porous particle layer with a thin hetero-oxide layer.[30),31)] Moreover, Wang et al.,[32)] reported that the electron life time was improved by using a band-structure matched double layer electrode composed of core–shell SnO_2–TiO_2 nano particles and ZnO nanoplates as the first and second layers, respectively.

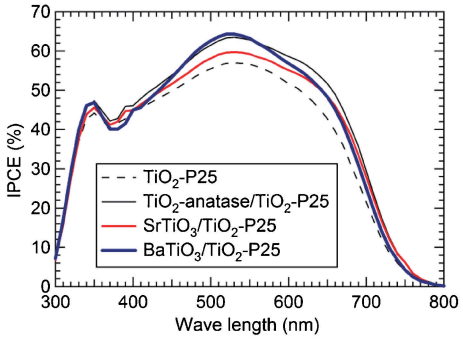

Fig. 7. IPCE curves of the DSCs composed of the single and double-layer electrodes.

$SrTiO_3/TiO_2$-P25 and $BaTiO_3/TiO_2$-P25 have the similar band structures as shown in Fig. 1. Therefore, the electron life times of $SrTiO_3/TiO_2$-P25 and $BaTiO_3/TiO_2$-P25 can be improved, resulting in the increase of the V_{OC}. In contrast, the V_{OC} of TiO_2-anatase/TiO_2-P25 was not enhanced due to the almost constant CB of TiO_2-anatase and TiO_2-P25.

The conversion efficiency of TiO_2-P25, TiO_2-anatase/TiO_2-P25, $SrTiO_3/TiO_2$-P25 and $BaTiO_3/TiO_2$-P25 were 5.12, 5.49, 5.32 and 5.71%, respectively. The DSCs using double-layer electrodes had larger conversion efficiencies than that of TiO_2-P25 single-layer electrode due to the enhancement of J_{SC} and V_{OC}. The largest conversion efficiency (5.71%) was obtained for the double-layer DSC using $BaTiO_3$. **Figure 7** shows IPCE curves of the prepared DSCs. Although the dye adsorptions of double-layer electrode were comparable to that of TiO_2-P25 (Table 1), their IPCE values were larger than that of TiO_2-P25 in all wavelength range from 400 to 800 nm. The enhancement is possibly due to the extended path of light by the two times thicker film of the double-layer electrodes than that of single-layer electrode. This resulted in the enhancement of IPCE in the all wavelength even with comparable dye adsorptions. Furthermore, the light confinement effect by the second layer composed of relatively large particles also contributed to the remarkable increase at ~650 nm.[11] These effects resulted in the increase of J_{SC}.

4. Conclusions

The double-layer electrodes composed of TiO_2-P25 first layer and $SrTiO_3$ or $BaTiO_3$ second layer were prepared to improve the performance of DSCs. $SrTiO_3/TiO_2$-P25 and $BaTiO_3/TiO_2$-P25 showed improved V_{OC} compared with DSCs using only TiO_2 either single or double layers. The V_{OC} improvement was probably attributed to (1) the inhibition of electron–hole recombination at the top side of TiO_2 layer, covered by the $SrTiO_3$ or $BaTiO_3$ second layer, and (2) the improved electron life time by the band structure matching. The larger J_{SC} were obtained for the DSCs using double-layer electrodes. The improvement is attributable to the extended light path by increase of the electrode's thickness and light confinement effect by the second layer with relatively large particles. As a result, the DSC using $BaTiO_3$ double-layer electrode had the largest conversion efficiency of 5.71% with an enhancement of 11.3% compared to that of TiO_2-P25 single-layer electrode.

Acknowlegement We thank to Dr. Tohru S. Suzuki at NIMS and Prof. Tamotsu Koyano at Univ. Tsukuba for the use of SEM and thank to Dr. Takeshi Yasuda at NIMS for the use of IPCE measurement system. We especially thank to the anonymous reviewer for helpful advice. We also thank to the OPEN FACILITY, Research Facility Center for Science and Technology, University of Tsukuba for the use of UV–Vis spectroscopy.

References

1) B. O'Regan and M. Grätzel, *Nature*, 353, 737–740 (1991).
2) S. Mathew, A. Yella, P. Gao, R. Humphry-Baker, B. F. E. Curchod, N. Ashari-Astani, I. Tavernelli, U. Rothlisberger, M. K. Nazeeruddin and M. Grätzel, *Nat. Chem.*, 6, 242–247 (2014).
3) A. Yella, H. W. Lee, H. N. Tsao, C. Y. Yi, A. K. Chandiran, M. K. Nazeeruddin, E. W. G. Diau, C. Y. Yeh, S. M. Zakeeruddin and M. Grätzel, *Science*, 334, 629–634 (2011).
4) Y. Chiba, A. Islam, Y. Watanabe, R. Komiya, N. Koide and L. Y. Han, *Jpn. J. Appl. Phys.*, 45, L638–L640 (2006).
5) F. Sauvage, D. Chen, P. Comte, F. Huang, L. P. Heiniger, Y. B. Cheng, R. A. Caruso and M. Grätzel, *ACS Nano*, 4, 4420–4425 (2010).
6) S. Ito, T. N. Murakami, P. Comte, P. Liska, C. Grätzel, M. K. Nazeeruddin and M. Grätzel, *Thin Solid Films*, 516, 4613–4619 (2008).
7) K. Kakiage, Y. Aoyama, T. Yano, T. Otsuka, T. Kyomen, M. Unnoc and M. Hayama, *Chem. Commun.*, 50, 6379–6381 (2014).
8) K. Kurotobi, Y. Toude, K. Kawamoto, Y. Fujimori, S. Ito, P. Chabera, V. Sundstrom and H. Imahori, *Chem.- Eur. J.*, 19, 17075–17081 (2013).
9) M. Grätzel, *J. Photochem. Photobiol., C*, 4, 145–153 (2003).
10) K. Nakata and A. Fujishima, *J. Photochem. Photobiol., C*, 13, 169–189 (2012).
11) Z. S. Wang, H. Kawauchi, T. Kashima and H. Arakawa, *Coodinat. Chem. Rev.*, 248, 1381–1389 (2004).
12) Q. F. Zhang, C. S. Dandeneau, X. Y. Zhou and G. Z. Cao, *Adv. Mater.*, 21, 4087–4108 (2009).
13) S. Gubbala, V. Chakrapani, V. Kumar and M. K. Sunkara, *Adv. Funct. Mater.*, 18, 2411–2418 (2008).
14) K. Sayama, H. Sugihara and H. Arakawa, *Chem. Mater.*, 10, 3825–3832 (1998).
15) H. D. Zheng, Y. Tachibana and K. Kalantar-zadeh, *Langmuir*, 26, 19148–19152 (2010).
16) Y. Diamant, S. G. Chen, O. Melamed and A. Zaban, *J. Phys. Chem. B*, 107, 1977–1981 (2003).
17) S. M. Yang, H. Z. Kou, K. Cheng and H. J. Wang, *Electrochim. Acta*, 55, 305–310 (2009).
18) A. Kitiyanan, S. Ngamsinlapasathian, S. Pavasupree and S. Yoshikawa, *Solid State Chem.*, 178, 1044–1048 (2005).
19) T. P. Brennan, J. T. Tanskanen, K. E. Roelofs, J. W. F. To, W. H. Nguyen, J. R. Bakke, I. Ding, B. E. Hardin, A. Sellinger, M. D. McGehee and S. F. Bent, *J. Phys. Chem. C*, 117, 24138–24149 (2013).
20) X. Lu, S. Ding, T. Lin, X. Mou, Z. Hong and F. Huang, *Dalton Trans.*, 41, 622–627 (2012).
21) M. Zhong, J. Shi, W. Zhang, H. Han and C. Li, *Mater. Sci. Eng., B*, 176, 1115–1122 (2011).
22) L. Zhang, Y. Shi, S. Peng, J. Lang, Z. Tao and J. Chen, *J. Photochem. Photobiol., A*, 197, 260–265 (2008).
23) Y. Okamoto and Y. Suzuki, *J. Ceram. Soc. Japan*, 122, 728–731 (2014).
24) S. Burnside, J. E. Moser, K. Brooks and M. Grätzel, *J. Phys. Chem. B*, 103, 9328–9332 (1999).
25) J. S. Jang, P. H. Borse, J. S. Lee, K. T. Lim, O. S. Jung, E. D. Jeong, J. S. Bae and H. G. Kim, *Bull. Korean Chem. Soc.*, 32, 95–99 (2011).
26) A. Bhardwaj, N. V. Burbure and G. S. Rohrer, *J. Am. Ceram. Soc.*, 93, 4129–4134 (2010).
27) Y. Wang, T. Chen, Y. Huang, T. Huang, Y. Lee, H. Chiu and C. Lee, *J. Chin. Chem. Soc.*, 60, 1437–1441 (2013).

28) N. Koide, A. Islam, Y. Chiba and L. Han, *J. Photochem. Photobiol., A*, 182, 296–305 (2006).
29) W. W. Xu, L. H. Hu, X. D. Luo, P. S. Liu and S. Y. Dai, *Chin. Phys. Lett.*, 29, 018401 (2012).
30) G. R. R. A. Kumara, K. Tennakone, V. P. S. Perera, A. Konno, S. Kaneko and M. Okuya, *J. Phys. D: Appl. Phys.*, 34, 868–873 (2001).
31) G. R. R. A. Kumara, K. Tennakone, I. R. M. Kottegoda, P. K. M. Bandaranayake, A. Konno, M. Okuya, S. Kaneko and K. Murakami, *Semicond. Sci. Technol.*, 18, 312–318 (2003).
32) Y. F. Wang, W. X. Zhao, X. F. Li and D. J. Li, *Electrochim. Acta*, 151, 399–406 (2015).